Large enhancement of spontaneous emission rates of InAs quantum dots in GaAs microdisks

W. Fang, J. Y. Xu, A. Yamilov, and H. Cao

Department of Physics and Astronomy, Northwestern University, Evanston, Illinois 60208-3112

Y. Ma and S. T. Ho

Department of Electrical and Computer Engineering, Northwestern University, Evanston, Illinois 60208-3118

G. S. Solomon

Department of Electrical Engineering, Stanford University, Stanford, California 94305

Received November 7, 2001

We have studied the enhancement of spontaneous emission rates for InAs quantum dots embedded in GaAs microdisks in a time-resolved photoluminescence experiment. Inhomogeneous broadening of the quantum dot energy levels and random spatial distribution of the quantum dots in a microdisk lead to a broad distribution of the spontaneous emission rates. Using a nonnegative least-norm algorithm, we extract the distribution of spontaneous emission rates from the temporal decay of emission intensity. The maximum spontaneous emission enhancement factor exceeds 10. © 2002 Optical Society of America

OCIS codes: 350.3950, 270.0270, 140.4780, 300.6280, 320.7120.

Control of spontaneous emission in a microcavity has many applications, e.g., improvement of the efficiency of light-emitting devices and generation of nonclassical states of light. A microcavity reduces the number of allowed optical modes but increases the vacuum field intensity in these resonant modes. The spontaneous emission outside the cavity resonance is suppressed, whereas the spontaneous emission within the cavity resonance is enhanced. For an emitter that has negligible linewidth and is ideally spatially and spectrally coupled to a cavity mode, its spontaneous emission rate is enhanced by the Purcell factor $F_p = 3Q(\lambda/n)^3/4\pi^2 V_{\text{eff}}$, where Q is the cavity quality factor, V_{eff} is the effective mode volume, λ is the emission wavelength, and n is the index of refraction.[1] Initial experiments of spontaneous emission control are performed on atoms. Recently, semiconductor quantum dots (QDs) attracted[2–8] much interest for spontaneous emission control. Owing to their discrete density of electronic states, self-assembled InGaAs QDs have an extremely narrow homogeneous linewidth.

QDs embedded in microdisks are ideal systems for spontaneous emission control.[9–11] The whispering gallery (WG) modes of microdisks have a low volume and a high quality factor.[12] The homogeneous linewidth of InAs QDs is smaller than the spectral width of WG modes. Thus, a large enhancement of the spontaneous emission rates should be expected for QDs coupled to WG modes. However, inhomogeneous broadening of QD energy levels and random spatial distribution of QDs in a microdisk lead to complications. The coupling of a QD to a WG mode depends both on spectral matching of the QD emission line with the WG mode frequency and on spatial overlap of the QD with the WG mode. Hence, the QDs with different emission frequencies and spatial locations undergo different spontaneous emission rate enhancement. The average enhancement factor is much less than the Purcell factor.[10] Recently, the Purcell effect of a single InAs QD in a GaAs microdisk was studied.[11] Although the frequency of the QD can be tuned into resonance with a WG mode, its location in the microdisk cannot be controlled. The spatial mismatch between the single QD and the WG mode reduces the spontaneous emission enhancement factor.

In this Letter we directly measure the lifetime of radiative decay of InAs QDs coupled to WG modes of GaAs microdisks. Using the nonnegative least-norm algorithm, we recover the distribution of spontaneous emission rates for an ensemble of QDs. The maximum enhancement factor of the spontaneous emission rate exceeds 10.

The QD sample is grown by molecular beam epitaxy. The structure consists of a GaAs buffer layer, 500-nm $Al_{0.7}Ga_{0.3}As$, 45-nm GaAs, two monolayer InAs QDs, and 45-nm GaAs. The areal density of InAs QDs is $\sim 10^{11}$ cm^{-2}. The photoluminescence (PL) spectrum of QDs at 5 K is centered around 970 nm with a FWHM of 20 nm.

The microdisks are fabricated by electron-beam lithography and two steps of wet etching.[13] The diameter of the disks is ~ 3 μm. The sample temperature is set at 5 K. A microdisk is optically excited by 200-fs pulses from a mode-locked Ti:sapphire laser with a repetition rate of 76 MHz. The excitation wavelength is fixed at 780 nm (1.59 eV). A microscope objective lens focuses the pump beam onto a single microdisk at normal incidence. The emission is collected from the side of the microdisk with a short achromatic lens. A beam splitter splits the collected emission into two. One half is dispersed by a 0.3-m monochromator with a 600-groove/mm grating and then enters a Hamamatsu streak camera for lifetime measurement. The temporal resolution is 17 ps. The other half is directed to a 0.5-m spectrometer with an 1800-groove/mm grating and is detected by a liquid-nitrogen-cooled CCD array detector for simultaneous spectral measurement. The spectral resolution is approximately 0.06 nm.

0146-9592/02/110948-03$15.00/0

Using the monochromator–streak camera system, we extracted the time traces of PL at various wavelengths. For wavelengths both shorter and longer than the cavity resonances, the PL curves exhibit monoexponential decay. The decay time, obtained from monoexponential curve fitting, is ~570 ps (curve A in Fig. 1). This value is close to the measured decay time of InAs QDs in the unprocessed sample. Curve B in Fig. 1 represents PL at 973.5 nm, which corresponds to the $TE_{13,2}$ mode. From the spectral linewidth of the $TE_{13,2}$ mode measured with the 0.5-m spectrometer, we find its Q value is around 3600. The InAs QDs located near the center of the disk have little spatial overlap with the $TE_{13,2}$ mode. Thus their coupling to the $TE_{13,2}$ mode is weak, even if their emission frequency is in resonance with the $TE_{13,2}$ mode. The collected PL at the wavelength of the $TE_{13,2}$ mode consists of two parts: the resonant part represents the emission of QDs into the $TE_{13,2}$ mode and the nonresonant part from the emission of uncoupled QDs. We curve fit the temporal decay of PL with a double-exponential function

$$I(t) = I_1 \exp[-(t - t_0)/t_1] + I_2 \exp[-(t - t_0)/t_2] + I_0.$$

The first term corresponds to the resonant part, the second term is the nonresonant part, the third term is the background noise. t_1 represents the decay time averaged over all coupled QDs, and t_2 is the off-resonant spontaneous emission decay time. According to the curve fit of PL decay at an off-resonance wavelength, the value of t_2 is set at 570 ps. The fitted curve is plotted in Fig. 1. The fitting result gives $t_1 = 150$ ps. Thus, the average enhancement factor for spontaneous emission rates of coupled QDs is 3.8.

Theoretically, the enhancement of a QD's spontaneous emission rate γ by a WG mode can be estimated as[14]

$$\frac{\gamma}{\gamma_0} = \frac{3Q(\lambda_c/n)^3}{4\pi^2 V_{\text{eff}}} \frac{\Delta\lambda_c{}^2}{4(\lambda - \lambda_c)^2 + \Delta\lambda_c{}^2} \frac{|\mathbf{E}(\mathbf{r})|^2}{|E_{\max}|^2} 2\eta^2, \quad (1)$$

where γ_0 is the spontaneous emission rate of the QD without the cavity; λ is the QD emission wavelength; λ_c and $\Delta\lambda_c$ are, respectively, the central wavelength and the linewidth of the WG mode; $\mathbf{E}(\mathbf{r})$ is the electric field amplitude of the WG mode at position $\mathbf{r}$ of the QD; and $E_{\max} = (\hbar\omega/2\epsilon_0 n^2 V_{\text{eff}})^{1/2}$. The first term in Eq. (1) is the Purcell factor. Its value is estimated to be 25 for the $TE_{13,2}$ mode. The second and third terms describe the spectral and spatial match between the QD and the WG mode. The factor of 2 comes from the twofold degeneracy of the WG mode. η describes the orientation match between the dipole of the QD and the polarization of the WG mode. Despite the large value of the Purcell factor, the spectral, spatial, and orientation mismatches lead to a significant reduction of the enhancement factor. Assuming uniform distribution of QDs in space and in spectrum, we estimate the average enhancement factor as

$$\left\langle \frac{\gamma}{\gamma_0} \right\rangle = F_p \left[\frac{1}{2\lambda_w} \int_{-\lambda_w}^{\lambda_w} \frac{\Delta\lambda_c{}^2}{4(\lambda - \lambda_c)^2 + \Delta\lambda_c{}^2} \, d\lambda \right] \times \left[\frac{1}{V} \int |f(\mathbf{r})|^2 d\mathbf{r} \right] 2\frac{1}{3}, \quad (2)$$

where λ_w is the FWHM of the WG mode and $f(\mathbf{r})$ is the envelope function of the electric field amplitude for the WG mode, whose norm is unity at the antinode of the electric field. For the $TE_{13,2}$ mode, the average enhancement factor is estimated to be 3.4, which is close to the experimental value.

Since the spontaneous emission enhancement factor depends on the spectral and spatial overlap of the QD with the WG mode, each QD in the microdisk undergoes a specific spontaneous emission rate enhancement. Hence, the spontaneous emission rates for the coupled QDs have a distribution. A more accurate way of describing the spontaneous emission enhancement than by use of the average enhancement factor is to introduce a distribution function $P(\gamma)$ for the spontaneous emission rate γ. The temporal evolution of emission intensity $I(t)$ at the frequency of a WG mode can be written as

$$I(t) = I_0 \int_0^\infty P(\gamma) \exp(-\gamma t) dt, \quad (3)$$

where $P(\gamma)$ is normalized: $\int_0^\infty P(\gamma) d\gamma = 1$. We numerically solve integral equation (3) to retrieve $P(\gamma)$ from the measured $I(t)$. We use the truncated singular value decomposition to find the distribution with minimal L_2 norm $\int_0^\infty [P(\Gamma)]^2 d\Gamma$.[15–17] The nonnegative constraint, $P(\Gamma) > 0$, is applied to the search for $P(\Gamma)$.

Figure 2 shows the distributions of the spontaneous emission rates $P(\gamma)$ recovered from on-resonance and off-resonance PL decay curves $I(t)$. Curves A and B represent $P(\gamma)$ at the off-resonance wavelength of 978 nm under the incident pump intensities

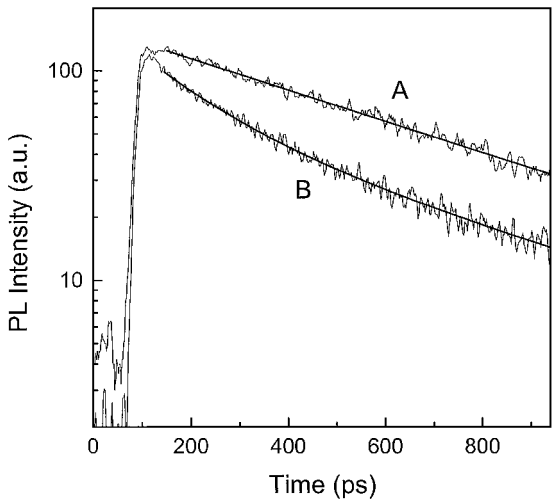

Fig. 1. Time-resolved PL curves at wavelengths of 977.7 nm (curve A) and 973.5 nm (curve B). The incident pump intensity is 4.2×10^2 W/cm^2. Curve A is fitted with a monoexponential decay function; curve B is fitted with a double-exponential decay function.

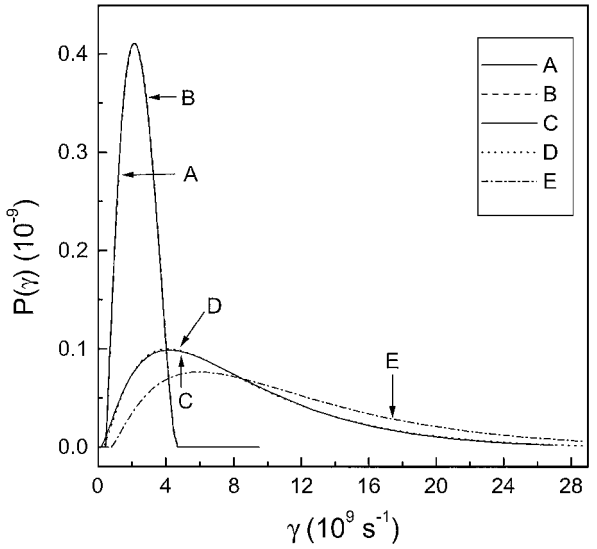

Fig. 2. Distributions $P(\gamma)$ of decay rates γ extracted from the PL curves at wavelengths of 978 nm (curves A and B) and 973.5 nm (curves C, D, and E). The incident pump intensities are A, 4.2×10^2; B, 1.3×10^3; C, 2.8×10^2; D, 4.2×10^2; E, 1.3×10^3 W/cm^2.

of 4.2×10^2 and 1.3×10^3 W/cm^2, respectively. Curves C, D, and E represent $P(\gamma)$ at the wavelength of the $TE_{13,2}$ mode under the incident pump intensities of 2.8×10^2, 4.2×10^2, and 1.3×10^3 W/cm^2, respectively. At the off-resonance wavelength, the distribution function is a narrow peak centered at ~2 GHz. The central decay rate corresponds to a decay time of ~500 ps. This value is close to the decay time obtained from the monoexponential curve fitting of the nonresonance PL curves. At the wavelength of the $TE_{13,2}$ mode, $P(\gamma)$ has a long tail at the higher decay rate, which indicates that the decay rates for some QDs are enhanced. The large decay rates can result from the spontaneous emission enhancement or the stimulated emission. In the absence of stimulated emission, the decay rate distribution $P(\gamma)$ should be independent of the pump intensity. As shown in Fig. 2, the on-resonance decay rate distribution at the pump intensity of 4.2×10^2 W/cm^2 (curve D) is almost identical to that at 2.8×10^2 W/cm^2 (curve C), which confirms that curves C and D represent the distribution of spontaneous emission rates. In other words, the 4.2×10^2-W/cm^2 pump intensity is low enough that the stimulated emission into the $TE_{13,2}$ mode is negligible. According to curves C and D, the spontaneous emission rates for some QDs exceed 20 GHz. The corresponding decay time is less than 50 ps. Therefore, the spontaneous emission enhancement factor for some QDs exceeds 10. When the pump intensity is increased to 1.3×10^3 W/cm^2, the on-resonance decay rate distribution changes and $P(\gamma)$ extends to a higher decay rate. The change of $P(\gamma)$ reveals the emergence of stimulated emission into the $TE_{13,2}$ mode. Note that at the same pump intensity of 1.3×10^3 W/cm^2, the off-resonance decay rate distribution (curve B) remains identical to that at 4.2×10^2 W/cm^2 (curve A). This means that stimulated emission does not exist in the off-resonance PL at 1.3×10^3 W/cm^2. Therefore, at the cavity resonant frequency, stimulated emission emerges at a much lower pump intensity, owing to the high Q of the WG mode.

An important issue in the measurement of spontaneous emission enhancement by a microcavity is elimination of stimulated emission. Some QDs have stronger coupling to the cavity mode, and stimulated emission could occur in them at a lower pumping intensity, where most QDs still spontaneously emit photons. Thus, it is difficult to estimate the pumping intensity when stimulated emission can be neglected for all the QDs. From the dependence of the decay rate distribution on the pumping intensity, we can identify the onset of stimulated emission for all the QDs, which thus eliminates the possibility of having stimulated emission in any QDs.

We thank E. P. Petrov and A. A. Goldin for providing us with valuable information on the algorithms for recovery of the fluorescence decay time distribution. This study is supported by the National Science Foundation under grant ECS-9800068. H. Cao's e-mail address is h-cao@northwestern.edu.

References

1. E. M. Purcell, Phys. Rev. **69,** 681 (1946).
2. J. M. Gerard, B. Sermage, B. Gayral, B. Legrand, E. Costard, and V. Thierry-Mieg, Phys. Rev. Lett. **81,** 1110 (1998).
3. L. A. Graham, D. L. Huffaker, Q. Deng, and D. G. Deppe, Appl. Phys. Lett. **72,** 1670 (1998).
4. L. A. Graham, D. L. Huffaker, and D. G. Deppe, Appl. Phys. Lett. **74,** 2408 (1999).
5. C. Santori, M. Pelton, G. S. Solomon, Y. Dale, and Y. Yamamoto, Phys. Rev. Lett. **86,** 1502 (2001).
6. M. Bayer, T. L. Reinecke, F. Weidner, A. Larionov, A. McDonald, and A. Forcel, Phys. Rev. Lett. **86,** 3168 (2001).
7. G. S. Solomon, M. Pelton, and Y. Yamamoto, Phys. Rev. Lett. **86,** 3903 (2001).
8. C. Becher, A. Kiraz, P. Michler, A. Imamoglu, W. V. Schoenfeld, P. M. Petroff, L. Zhang, and E. Hu, Phys. Rev. B **63,** R121312 (2001).
9. P. Michler, A. Kiraz, C. Becher, W. V. Schoenfeld, P. M. Petroff, L. Zhang, E. Hu, and A. Imamoglu, Science **290,** 2282 (2000).
10. B. Gayral, J. M. Gerard, B. Sermage, A. Lemaitre, and C. Dupuis, Appl. Phys. Lett. **78,** 2828 (2001).
11. A. Kiraz, P. Michler, C. Becher, G. Gayral, A. Imamoglu, L. Zhang, E. Hu, W. V. Schoenfeld, and P. M. Petroll, Appl. Phys. Lett. **78,** 3932 (2001).
12. B. Gayral, J. M. Gerard, A. Lemaitre, C. Dupuis, L. Manin, and J. L. Pelouard, Appl. Phys. Lett. **75,** 1908 (1999).
13. H. Cao, J. Y. Xu, W. H. Xiang, Y. Ma, S.-H. Chang, S. T. Ho, and G. S. Solomon, Appl. Phys. Lett. **76,** 3519 (2000).
14. J. M. Gerard and B. Gayral, J. Lightwave Technol. **17,** 2089 (1999).
15. D. M. Gakamsky, A. A. Goldin, E. P. Petrov, and A. N. Rubinov, Biophys. Chem. **44,** 47 (1992).
16. A. A. Goldin, Opt. Spektrosk. (USSR) **71,** 485 (1991).
17. E. P. Petrov, V. N. Bogomolov, I. I. Kalosha, and S. V. Gaponenko, Acta. Phys. Pol. A **94,** 761 (1998).